Photoplethysmography pulse rate variability as a surrogate measurement of heart rate variability during non-stationary conditions



2010 Physiol. Meas. 31 1271

(http://iopscience.iop.org/0967-3334/31/9/015)

IOP PUBLISHING PHYSIOLOGICAL MEASUREMENT

Physiol. Meas. **31** (2010) 1271–1290 doi:10.1088/0967-3334/31/9/015

# Photoplethysmography pulse rate variability as a surrogate measurement of heart rate variability during non-stationary conditions

**E Gil[1,2], M Orini[1,2,3], R Bailón[1,2], J M Vergara[2,4], L Mainardi[3] and P Laguna[1,2]**

[1] Communications Technology Group, Aragón Institute of Engineering Research, University of Zaragoza, Zaragoza, Spain
[2] CIBER de Bioingeniería, Biomateriales y Nanomedicina (CIBER-BBN), Zaragoza, Spain
[3] Department of Bioengineering, Politecnico di Milano, Milano, Italy
[4] Sleep Department, Miguel Servet Children Hospital, Zaragoza, Spain

E-mail: edugilh@unizar.es

Received 28 March 2010, in final form 22 July 2010
Published 11 August 2010
Online at stacks.iop.org/PM/31/1271

**Abstract**

In this paper we assessed the possibility of using the pulse rate variability (PRV) extracted from the photoplethysmography signal as an alternative measurement of the HRV signal in non-stationary conditions. The study is based on analysis of the changes observed during a tilt table test in the heart rate modulation of 17 young subjects. First, the classical indices of HRV analysis were compared to the indices from PRV in intervals where stationarity was assumed. Second, the time-varying spectral properties of both signals were compared by time-frequency (TF) and TF coherence analysis. Third, the effect of replacing PRV with HRV in the assessment of the changes of the autonomic modulation of the heart rate was considered. Time-invariant HRV and PRV indices showed no statistically significant differences ($p > 0.05$) and high correlation (>0.97). Time-frequency analysis revealed that the TF spectra of both signals were highly correlated ($0.99 \pm 0.01$); the difference between the instantaneous power, in the LF and HF bands, obtained from HRV and PRV was small ($<10^{-3}$ s$^{-2}$) and their temporal patterns were highly correlated ($0.98 \pm 0.04$ and $0.95 \pm 0.06$ in the LF and HF bands, respectively) and TF coherence in the LF and HF bands was high ($0.97 \pm 0.04$ and $0.89 \pm 0.08$, respectively). Finally, the instantaneous power in the LF band was observed to significantly increase during head-up tilt by both HRV and PRV analysis. These results suggest that although some differences in the time-varying spectral indices extracted from HRV and PRV exist, mainly in the HF band associated with respiration, PRV could be used as a surrogate of HRV during non-stationary conditions, at least during the tilt table test.

  

Keywords: pulse rate variability, heart rate variability, photoplethysmography, tilt test, time-frequency analysis, time-frequency coherence

(Some figures in this article are in colour only in the electronic version)

## 1. Introduction

Pulse photoplethysmography (PPG), introduced by Hertzman (1938), is a simple and useful method for measuring the relative blood volume changes in the microvascular bed of peripheral tissues and evaluating peripheral circulation. This signal is obtained through non-invasive pulse oximetry systems and is based on blood light absorption (Yoshiya *et al* 1980, Mendelson, 1992). The PPG waveform contains both a dc and an ac component. The first one is due to the non-pulsatile blood volume component and the attenuation at the tissues surrounding the arteries, which produces a signal that changes slowly. The second one is attributable to the pulsatile component of the vessels, i.e. the arterial pulse, which is caused by the heartbeat pumping. PPG has been applied in many different clinical settings, including the monitoring of blood oxygen saturation, heart rate, blood pressure, cardiac output and respiration (Allen 2007). Given its simplicity, low-cost and that it is widely used in the clinical routine, it is desirable to maximize the PPG potential by exploring additional measurements which can be derived from it. It is worth noting that oximetry systems have the potentiality of providing multiple information using only one sensor, making its use simpler, more comfortable and cheaper than multiple sensor devices.

It is generally accepted that PPG can provide valuable information about the cardiovascular system. The autonomic influences on the PPG signal have been analysed in several studies (Bernardi *et al* 1996, Nitzan *et al* 1998, Khanokh *et al* 2004), and recently pulse rate variability (PRV) extracted from PPG has been studied as a potential surrogate of heart rate variability (HRV) (Lu *et al* 2008, 2009a, Hayano *et al* 2005, Selvaraj *et al* 2008, Charlot *et al* 2009). HRV analysis is one of the most widely used non-invasive techniques for the evaluation of the autonomic nervous system (ANS). The use of PRV as a surrogate of HRV could be useful in applications where ECG is not available, or when it is beset with electrical artefacts (Martin *et al* 2003). Moreover, since PPG also allows us to derive physiological parameters such as blood oxygenation and ventilatory rate, the use of PRV instead of HRV could be particularly suitable in those applications where the simultaneous acquisition of many signals is required, as for example in sleep disorder studies, mainly for ambulatory sleep studies. The main difference between HRV and PRV is the time the pulse wave takes to travel from the heart to the finger. This time is called the pulse transit time (PTT) and is typically measured as the difference between the peak of the R-wave on the ECG and the peak value of the corresponding pulse in the finger pad measured by PPG. PTT, which is tie-related to arterial compliance and blood pressure, changes beat to beat (Chen *et al* 2000, Ma and Zhang 2006, Naschitz *et al* 2004, Foo and Lim 2006, Gil *et al* 2010). Thus, PRV is also affected by the variability in the PTT, i.e. the beat-to-beat changes in the pulse wave velocity.

All the studies exploring the possibility of using PRV as an alternative measurement of HRV have been performed in stationary conditions using time-invariant analysis and generally showed that PRV is a good surrogate of HRV. However, there are many situations where significant changes in autonomic balance occur, as during orthostatic test, Valsalva manoeuver, exercise stress testing and after pharmacologic interventions, which involve non-stationary processes. In such situations, the use of PRV as an alternative measurement of HRV could be

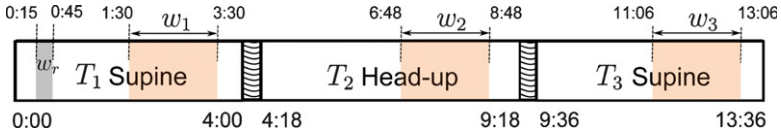


**Figure 1.** Head-up tilt test protocol. Table takes 18 s to tilt during transitions, marked as the lined area. The windows $w_1$, $w_2$ and $w_3$ define the intervals where stationarity was assumed and time-invariant analysis was performed, see section 2.2, and $w_r$ defines the interval where the baseline was estimated for time-invariant physiological analysis, see section 2.4.

of great interest. In this paper, we focused the study on the tilt table test. In this test, after head-up tilt, subjects undergo a progressive orthostatic stress and blood pressure is maintained thanks to cardiovascular regulation (Julu *et al* 2003), which involves an increase in heart rate and a constriction of the blood vessels in the legs. This slight tachycardia and vasoconstriction are the result of sympathetic activation and vagal withdrawal (Montano *et al* 1994). When the supine position is restored, heart rate and vasoconstriction return to previous basal values together with sympathetic tone.

The aim of this work is to evaluate the usefulness of PRV as a surrogate of HRV analysis during non-stationary conditions, in particular, during the tilt table test. Time-frequency (TF) and TF coherence analysis were performed to asses whether the PRV can be used in the analysis of the autonomic modulation of heart rate in non-stationary conditions.

## 2. Material and methods

### *2.1. Data and signal preprocessing*

Seventeen volunteers (age 28.5 ± 2.8 years, 11 males) underwent a head-up tilt table test according to the following protocol: 4 min in early supine position ($T_1$), 5 min tilted head-up to an angle of 70° ($T_2$) and 4 min back to later supine position ($T_3$), see figure 1. Table 1 shows database information, where blood pressure from the finger was measured during early supine position, $T_1$.

The PPG signal was recorded from the index finger using the Biopac's PPG100C amplifier with the TSD200 transducer with a sampling frequency of 250 Hz, whereas the standard lead V4 ECG signal was recorded using the Biopac's ECG100C amplifier and disposable Ag–AgCl electrodes with a sampling frequency of 1000 Hz. The MP 150 (BIOPAC Systems), a computer-based data acquisition system with the software AcqKnowledge® 3.9.0, was used to acquire both signals simultaneously.

Beats from ECG and pulses from PPG were detected to generate heart and pulse rate time series. The temporal location of each R-wave in the ECG $\left(t_{\mathrm{E}_j}\right)$ was automatically determined using the algorithm described by Martinez *et al* (2004). The PPG signal was interpolated using cubic splines increasing the resolution in time up to an equivalent sampling rate of 1000 Hz to match the temporal resolution of both signals. Then, the temporal location of each pulse wave in PPG $\left(t_{\mathrm{P}_j}\right)$ was detected as the maximum of the PPG signal within the interval $\left[t_{\mathrm{E}_j} + 150\ \mathrm{ms},\ t_{\mathrm{E}_{j+1}}\right]$; see figure 2. In addition, a PPG artefact detector (Gil *et al* 2008) was applied to suppress pulses from PPG corresponding to artefacts, and beat and pulse detections were manually supervised. Then, the effect of abnormal beats on both heart and pulse rate was corrected by applying a methodology based on the integral pulse frequency modulation model (Mateo and Laguna 2003). The heart rate and pulse rate signals, $d_{\mathrm{HR}}(t)$ and $d_{\mathrm{PR}}(t)$,

**Table 1.** Database information

| Subject | Age | Sex | SBP (mmHg)[a] | DBP (mmHg)[a] |
|---|---|---|---|---|
| s1 | 28 | Female | $113.5 \pm 5.4$ | $64.2 \pm 3.1$ |
| s2 | 26 | Male | $125.2 \pm 6.6$ | $82.3 \pm 4.1$ |
| s3 | 27 | Male | $69.1 \pm 4.7$ | $34.7 \pm 3.7$ |
| s4 | 27 | Male | $120.1 \pm 5.5$ | $69.5 \pm 2.6$ |
| s5 | 27 | Male | $122.6 \pm 6.9$ | $61.1 \pm 4.3$ |
| s6 | 34 | Female | $124.5 \pm 6.4$ | $64.5 \pm 2.9$ |
| s7 | 27 | Female | $118.1 \pm 5.7$ | $43.2 \pm 3.1$ |
| s8 | 31 | Female | $104.6 \pm 5.3$ | $59.2 \pm 2.3$ |
| s9 | 26 | Female | $117.1 \pm 2.8$ | $60.5 \pm 2.2$ |
| s10 | 29 | Male | $130.4 \pm 6.5$ | $86.9 \pm 2.6$ |
| s11 | 26 | Female | $95 \pm 2.7$ | $48.5 \pm 2.7$ |
| s12 | 24 | Male | $105.5 \pm 7.1$ | $67.5 \pm 3.1$ |
| s13 | 30 | Male | $104.9 \pm 7.6$ | $56.2 \pm 3.2$ |
| s14 | 31 | Male | $104.9 \pm 4.1$ | $54 \pm 3.2$ |
| s15 | 34 | Male | $124.5 \pm 3.9$ | $78.2 \pm 2.6$ |
| s16 | 29 | Male | – | – |
| s17 | 30 | Male | $137.9 \pm 3.6$ | $74.7 \pm 2.1$ |
| MEAN | $28.5 \pm 2.8$ | | $113.6 \pm 16.4$ | $62.8 \pm 14.0$ |

[a] Blood pressure was measured from the finger without height correction during the early supine position.

respectively, were obtained by using a fifth-order spline interpolation at 4 Hz of the inverse interval functions (IIF) $d_{\mathrm{IIF}}(t_j)$:

$$d_{\mathrm{IIF}}^{\mathrm{ECG}}\left(t_{\mathrm{E}_j}\right) = \frac{1}{\left(t_{\mathrm{E}_j} - t_{\mathrm{E}_{j-1}}\right)} \tag{1}$$

$$d_{\mathrm{IIF}}^{\mathrm{PPG}}\left(t_{\mathrm{P}_j}\right) = \frac{1}{\left(t_{\mathrm{P}_j} - t_{\mathrm{P}_{j-1}}\right)}. \tag{2}$$

Finally, the HRV and PRV signals, $d_{\mathrm{HRV}}(t)$ and $d_{\mathrm{PRV}}(t)$, were calculated by suppressing the time-varying mean heart/pulse rate from $d_{\mathrm{HR}}(t)$ and $d_{\mathrm{PR}}(t)$, respectively. The mean heart/pulse rates were estimated by low-pass filtering $d_{\mathrm{HR}}(t)$ and $d_{\mathrm{PR}}(t)$, respectively, with a cut-off frequency of 0.03 Hz in order to suppress the dc component of the heart/pulse rates.

Using equations (1) and (2), it is possible to describe the relationship between the HRV from ECG and the PRV from PPG as

$$\begin{aligned} d_{\mathrm{IIF}}^{\mathrm{PPG}}\left(t_{\mathrm{P}_j}\right) &= \frac{1}{\left(t_{\mathrm{P}_j} - t_{\mathrm{P}_{j-1}}\right)} = \frac{1}{\left(t_{\mathrm{E}_j} + \tau_{\mathrm{PTT}_j} + \xi_j\right) - \left(t_{\mathrm{E}_{j-1}} + \tau_{\mathrm{PTT}_{j-1}} + \xi_{j-1}\right)} \\ &= \frac{1}{\left(t_{\mathrm{E}_j} - t_{\mathrm{E}_{j-1}}\right)} \cdot \frac{1}{1 + \frac{\tau_{\mathrm{PTT}_j} - \tau_{\mathrm{PTT}_{j-1}} + \xi_j - \xi_{j-1}}{t_{\mathrm{E}_j} - t_{\mathrm{E}_{j-1}}}} \\ &\approx \frac{1}{\left(t_{\mathrm{E}_j} - t_{\mathrm{E}_{j-1}}\right)} \left[1 - \frac{\tau_{\mathrm{PTT}_j} - \tau_{\mathrm{PTT}_{j-1}} + \xi_j - \xi_{j-1}}{t_{\mathrm{E}_j} - t_{\mathrm{E}_{j-1}}}\right] \\ &= d_{\mathrm{IIF}}^{\mathrm{ECG}}\left(t_{\mathrm{E}_j}\right)\left[1 - \left(\Delta_{\mathrm{PTT}_j}\left(t_{\mathrm{E}_j}\right) + \Delta_{\xi_j}\left(t_{\mathrm{E}_j}\right)\right) \cdot d_{\mathrm{IIF}}^{\mathrm{ECG}}\left(t_{\mathrm{E}_j}\right)\right], \end{aligned} \tag{3}$$

where $\tau_{\mathrm{PTT}_j}$ is the PTT for the $j$th beat, $\xi_j$ is a stochastic variable which accounts for errors in the location of $t_{\mathrm{P}_j}$ because the fiducial point on the PPG is much less definite than the

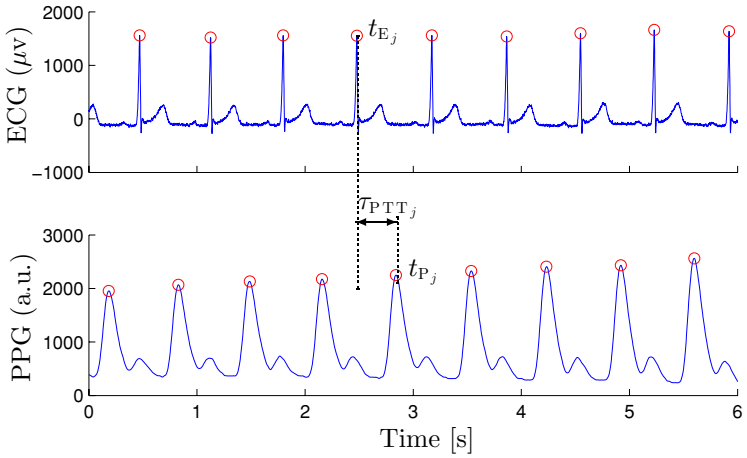


**Figure 2.** Beat and pulse detection example. Red circles correspond to $t_{E_j}$ and $t_{P_j}$.

R peak of ECG, while $\Delta_{PTT_j}(t_{E_j}) = \tau_{PTT_j} - \tau_{PTT_{j-1}}$ and $\Delta_{\xi_j}(t_{E_j}) = \xi_j - \xi_{j-1}$ are the PTT and the location error variabilities respectively. Note that in (3) it has been assumed that $(\Delta_{PTT_j}(t_{E_j}) + \Delta_{\xi_j}(t_{E_j})) \ll t_{E_j} - t_{E_{j-1}}$, and $t_{E_j}$ has no temporal jitter. The beat-to-beat difference between HRV and PRV is then

$$d_{IIF}^{PPG}(t_{P_j}) - d_{IIF}^{ECG}(t_{E_j}) = -(\Delta_{PTT_j}(t_{E_j}) + \Delta_{\xi_j}(t_{E_j})) \cdot (d_{IIF}^{ECG}(t_{E_j}))^2. \tag{4}$$

To test the isolated effect of $\xi_j$ and to indirectly assess the role played by PPT in equation (4), a simulation study was carried out. The difference between HRV and simulated PRV ($PRV_s$) is only due to the jitter in the PPG fiducial point. This is equivalent to write $t_{PS_j} = t_{E_j} + \xi_j$. Noise, $\xi_j$, was modelled by zero-mean discrete uniform distributions and varying standard deviation. The IIF for simulated PPG signals, $d_{IIF}^{PPG_s}(t_{P_{s_j}})$, were computed for all patients:

$$d_{IIF}^{PPG_s}(t_{P_{s_j}}) = \frac{1}{(t_{P_{s_j}} - t_{P_{s_{j-1}}})} = \frac{1}{(t_{E_j} + \xi_j) - (t_{E_{j-1}} + \xi_{j-1})}. \tag{5}$$

The simulated PRV signals $d_{PRV_s}(t)$ were obtained after interpolation and dc suppression as previously described for obtaining the HRV and PRV signals.

### 2.2. *Time-invariant analysis*

Pearson's correlation coefficient, defined as

$$\rho = \frac{C(\phi^X(j), \phi^Y(j))}{\sqrt{C(\phi^X(j), \phi^X(j))C(\phi^Y(j), \phi^Y(j))}}, \qquad X, Y \in \{HRV, PRV\}, \tag{6}$$

was used to quantify the linear strength between the HRV and PRV signals, as well as between several indices derived from HRV and PRV. In (6), $C$ represents the covariance operator, while $\phi(j)$ is a general function of the independent variable $j$ (which can represent subjects, time instants or frequency).

First, Pearson's correlation coefficient, $\rho_d(k)$, between the variability signals $\phi^X(t) = d_{HRV}(t)$ and $\phi^Y(t) = d_{PRV}(t)$ was calculated for each subject $k$ to evaluate their linear relationship. Then, a classical time-invariant analysis was performed in three windows ($w_1$, $w_2$ and $w_3$) where stationarity is assumed. These windows had a length of 2 min and finished 30 s before any transition during the tilt-test; see figure 1.

The power spectral density of the HRV exhibits oscillations related to the parasympathetic and sympathetic activities. The range between 0.003 and 0.04 Hz (very low-frequency component, VLF) takes account of long-term regulation mechanisms. The range between 0.04 and 0.15 Hz (low-frequency component, LF) represents both sympathetic and parasympathetic modulation, although an increase in its power is generally associated with a sympathetic activation. However, even nowadays there is some controversy about the contribution of each autonomic branch to this frequency band. The range between 0.15 and 0.4 Hz (high-frequency component, HF) corresponds to parasympathetic modulation and is synchronous with the respiratory rate. Finally, the ratio between the power in the LF and HF bands is an index to evaluate the sympatho–vagal balance controlling the heart rate (Pagani *et al* 1986, Malliani *et al* 1991). Classical time domain and frequency domain indices were estimated in each window from both HRV and PRV (Task Force 1996).

- Time domain. Mean normal to normal interval (NN), standard deviation of NN intervals (SDNN), root mean square of successive differences of adjacent NN intervals (RMSSD) and percentage of pairs of adjacent NN intervals differing by more than 50 ms (pNN50) were estimated.
- Frequency domain. The fast Fourier transform algorithm with a frequency resolution of 0.0019 Hz was applied to $d_{\mathrm{HRV}}(t)$ and $d_{\mathrm{PRV}}(t)$ and the power in the low-frequency band ($P_{\mathrm{LF}}$), high-frequency band ($P_{\mathrm{HF}}$) and the LF to HF ratio ($R_{\mathrm{LF/HF}}$) were estimated.

Each index from PRV ($I^{\mathrm{PRV}}(k)$) was compared to the same index from HRV ($I^{\mathrm{HRV}}(k)$) for each subject $k$, with $I \in \{\mathrm{NN}, \mathrm{SDNN}, \mathrm{RMSSD}, \mathrm{pNN50}, P_{\mathrm{LF}}, P_{\mathrm{HF}}, R_{\mathrm{LF/HF}}\}$. Three indices were then estimated.

(1) The difference between the indices from HRV and PRV: $\delta_{\mathrm{I}}(k) = I^{\mathrm{PRV}}(k) - I^{\mathrm{HRV}}(k)$.
(2) The $p$-value of Student's $t$-test, used to assess whether the indices $I^{\mathrm{PRV}}(k)$ and $I^{\mathrm{HRV}}(k)$ were statistically different. Before analysis, the values of all variables were examined for deviations from normality by the Kolmogorov–Smirnov test, finding in all cases that the hypothesis of normality could not be rejected ($p > 0.05$).
(3) Pearson's correlation coefficient, $\rho_{\mathrm{I}}$, between the indices $\phi^{\mathrm{X}}(k) = I^{\mathrm{HRV}}(k)$ and $\phi^{\mathrm{Y}}(k) = I^{\mathrm{PRV}}(k)$ was used to measure their linear relationship.

### 2.3. *Time-varying analysis*

The smoothed pseudo Wigner–Ville distribution (SPWVD) was used to estimate the time-varying spectral properties of the HRV and PRV signals, as well as to perform TF coherence analysis. The cross-SPWVD of the signals $x(t)$ and $y(t)$ is defined as (Hlawatsch 1991, Martin and Flandrin 1985)

$$S_{x,y}(t, f) = \int_{-\infty}^{\infty}\int_{-\infty}^{\infty} \mathcal{K}(\tau, \nu) A_{x,y}(\tau, \nu)\, \mathrm{e}^{j2\pi(t\nu - f\tau)} \mathrm{d}\nu\, \mathrm{d}\tau \tag{7}$$

$$A_{x,y}(\tau, \nu) = \int_{-\infty}^{\infty} x\left(t + \frac{\tau}{2}\right) y^*\left(t - \frac{\tau}{2}\right) \mathrm{e}^{-j2\pi\nu t} \mathrm{d}t, \tag{8}$$

where $A_{x,y}(\tau, \nu)$ is the narrow band symmetric ambiguity function (AF) of the signals $x(t)$ and $y(t)$. The AF quantifies the TF correlation between $x(t)$ and $y(t)$ in the *delay–doppler frequency* domain $(\tau, \nu)$ and can be seen as the 2D Fourier transform of the Wigner–Ville distribution. The kernel $\mathcal{K}(\tau, \nu)$ is a 2D weighting function which performs the TF low-pass filtering necessary to suppress the interference terms which reduce the

readability of the Wigner–Ville distribution. The complex analytic signal representations $a_{\mathrm{HRV}}(t)$ and $a_{\mathrm{PRV}}(t)$ of the original real signals $d_{\mathrm{HRV}}(t)$ and $d_{\mathrm{PRV}}(t)$, respectively, were used in (7)–(8) in order to further reduce the interference terms (Martin and Flandrin 1985). We choose as kernel $\mathcal{K}(\tau, \nu)$ an elliptical exponential function defined as (Costa and Boudreau-Bartels 1995, Orini *et al* 2009)

$$\mathcal{K}(\tau, \nu; \tau_0, \nu_0) = \exp\left\{-\pi\left[\left(\frac{\nu}{\nu_0}\right)^2 + \left(\frac{\tau}{\tau_0}\right)^2\right]^{\frac{1}{2}}\right\}. \tag{9}$$

The kernel's iso-contours are ellipsis whose major axis length, i.e. the bandwidth of the TF low-pass filter, depends on the parameters $\tau_0$ and $\nu_0$. The parameters $\tau_0$ and $\nu_0$ were selected to have a frequency resolution of 0.0313 Hz and a time resolution of 15 s. The time and frequency resolutions were estimated as the full width at half maximum of the SPWVD of a pure sinus and of a temporal impulse, respectively. For each subject $k$, the temporal evolution of the power content of HRV and PRV within each frequency band, $P_{\mathrm{B}}^{\mathrm{X}}(k, t)$, with $\mathrm{X} \in \{\mathrm{HRV}, \mathrm{PRV}\}$, was obtained integrating $S_x(t, f)$ in the frequency bands $\mathrm{B} \in \{\mathrm{LF}, \mathrm{HF}\}$. The similarity between the temporal evolution of $d_{\mathrm{HRV}}(t)$ and $d_{\mathrm{PRV}}(t)$ was assessed by means of four indices.

(1) Pearson's correlation coefficient, $\rho_{\mathrm{I}}(k)$, between $\phi^{\mathrm{X}}(t) = P_{\mathrm{B}}^{\mathrm{HRV}}(k, t)$ and $\phi^{\mathrm{Y}}(t) = P_{\mathrm{B}}^{\mathrm{PRV}}(k, t)$, and between $\phi^{\mathrm{X}}(t) = R_{\mathrm{LF/HF}}^{\mathrm{HRV}}(k, t)$ and $\phi^{\mathrm{Y}}(t) = R_{\mathrm{LF/HF}}^{\mathrm{PRV}}(k, t)$.
(2) The difference between the instantaneous power of the two signals within each frequency band: $\delta_{\mathrm{B}}(k, t) = P_{\mathrm{B}}^{\mathrm{PRV}}(k, t) - P_{\mathrm{B}}^{\mathrm{HRV}}(k, t)$. This index is used to compare the temporal evolution of the spectral content of the signals.
(3) Pearson's correlation coefficient, $\rho_{\mathrm{S}}(k, t)$, between the instantaneous spectra of the two signals is estimated at every time instant $t = t_0$ as in (6) with $\phi^{\mathrm{X}}(f) = S_{a_{\mathrm{HRV}}}(t_0, f)$ and $\phi^{\mathrm{Y}}(f) = S_{a_{\mathrm{PRV}}}(t_0, f)$. This index is used to assess whether the signals are characterized by a similar distribution of energy with frequency.
(4) The quadratic TF coherence between the two signals within each frequency band estimated as (White and Boashash 1990, Orini *et al* 2009)

$$\gamma^2(t, f) = \frac{S_{x,y}(t, f) S_{x,y}^*(t, f)}{S_x(t, f) S_y(t, f)}; \qquad x, y \in \{a_{\mathrm{HRV}}(t), a_{\mathrm{PRV}}(t)\}. \tag{10}$$

TF coherence gives a continuous quantification of spectral coherence over time, being 1 in epochs characterized by perfect linear coupling and zero when the two signals are completely uncorrelated. From $\gamma^2(t, f)$, we obtained the band coherence $\gamma_{\mathrm{B}}^2(k, t)$ by averaging $\gamma^2(t, f)$ in each spectral band for each subject $k$.

The same indices were used for assessing the similarity between the temporal evolution of $d_{\mathrm{HRV}}(t)$ and $d_{\mathrm{PRV_s}}(t)$ for the simulation study.

### *2.4. Physiological analysis*

The tilt table test provokes changes in the autonomic modulation of the heart rate and is used to study the cardiovascular control (Julu *et al* 2003, Montano *et al* 1994). In this section, we assess the effect of replacing the HRV estimation from the ECG with the PRV estimation from the PPG, when the tilt table test is used to evaluate changes in the autonomic modulation of the heart rate.

In time-invariant analysis, Student's $t$-test was performed to compare the variations of the spectral indices $\left(P_{\mathrm{B}}^{\mathrm{X}}(k)\right)$ among the windows $w_1$, $w_2$ and $w_3$, estimated from both HRV and PRV signals. In time-varying analysis, we are interested in continuously monitoring the changes produced in the autonomic modulation of the heart rate during the tilt test. To this

end we quantified the statistical differences between the baseline power content $\overline{P_{\mathrm{B}}^{\mathrm{X}}}(k)$ and the power content at $t_0$, $P_{\mathrm{B}}^{\mathrm{X}}(k, t_0)$, by iteratively performing Student's $t$-test. The baseline power content $\overline{P_{\mathrm{B}}^{\mathrm{X}}}(k)$ was estimated by averaging $P_{\mathrm{B}}^{\mathrm{X}}(k, t)$ in a reference window $w_r$, selected at $T_1$ from 15 to 45 s (see figure 1). As a result of the test we obtained a time-varying $p$-value, $p_{\mathrm{B}}^{\mathrm{X}}(t)$, for both HRV and PRV signals. The normality of the distributions was tested by the Kolmogorov–Smirnov test, finding that the hypothesis of normality could not be rejected ($p > 0.05$) in 93% of the time.

## 3. Results

### *3.1. Time-invariant analysis*

The correlation between $d_{\mathrm{HRV}}(t)$ and $d_{\mathrm{PRV}}(t)$, $\rho_{\mathrm{d}}(k)$, was $0.964 \pm 0.030$ (mean $\pm$ S.D.). The mean delay of $d_{\mathrm{PRV}}(t)$ with respect to $d_{\mathrm{HRV}}(t)$, introduced by the pulse wave travel to the periphery, was taken into account in the estimation of the parameter $\rho_{\mathrm{d}}(k)$, so both signals were aligned. Table 2 and figure 3 show the comparison of classical time and frequency indices derived from HRV and PRV within each analysis window. All the indices derived from PRV presented similar values to the indices derived from HRV as proved by the statistical test that showed no significant differences between the indices from HRV and PRV ($p > 0.05$). In addition, as shown in table 2, correlation coefficients indicated a strong correlation ($\rho_{\mathrm{I}} > 0.97$) for all indices but one ($R_{\mathrm{LF/HF}}$ in $w_2$).

### *3.2. Time-varying analysis*

The results of TF and TF coherence analysis for a subject (subject $k = 17$, male, 30 years old) are reported in figure 4. Heart and pulse rates are reported in panel (a). The TF distributions of the HRV and PRV signals are shown in panels (b)–(c). The temporal evolution of the instantaneous power, within the LF and HF bands, $P_{\mathrm{B}}^{\mathrm{X}}(k = 17, t)$, is reported in panel (d). Note that, as also shown in panels (b)–(c), the spectral properties of the HRV and PRV signals did follow the same trend. The main difference lies in the slight increase of $P_{\mathrm{HF}}^{\mathrm{PRV}}(k = 17, t)$ with respect to $P_{\mathrm{HF}}^{\mathrm{HRV}}(k = 17, t)$, which was more pronounced during tilt. Panel (e) shows the correlation coefficient between the instantaneous spectra of the two signals, $\rho_{\mathrm{S}}(k = 17, t)$. The results of the TF coherence analysis are reported in panels (f)–(g). The quadratic TF coherence $\gamma^2(t, f)$, reported in panel (f), shows that during $T_1$ and $T_3$ the two signals presented almost a perfect correlation for all frequencies. Around 320 s TF coherence decreased due to artefacts on the PPG signal (marked as black crosses). Finally, the temporal evolution of the band coherence $\gamma_{\mathrm{B}}^2(k = 17, t)$, shown in panel (g), confirms the previous observations: HRV and PRV had an almost identical TF structure, at least in the LF band. It is worth noting that this is a borderline case: subject $k = 17$ had one of the highest $\delta_{\mathrm{HF}}(k, t)$ and the lowest $\gamma_{\mathrm{HF}}^2(k, t)$ in $T_2$.

Table 3 shows that the index $\rho_{\mathrm{I}}(k)$, with $I \in \{P_{\mathrm{LF}}(k, t), P_{\mathrm{HF}}(k, t), R_{\mathrm{LF/HF}}(k, t)\}$, was close to 1 for almost all subjects. Global results, obtained by averaging among subjects the indices presented in section 2.3, are reported in figure 5. In panels (a)–(b), the instantaneous power within each frequency band from HRV and PRV and the corresponding instantaneous difference are shown, respectively. Note that averaged $P_{\mathrm{B}}^{\mathrm{HRV}}(k, t)$ and $P_{\mathrm{B}}^{\mathrm{PRV}}(k, t)$ over subjects presented the same temporal patterns, even if with a bias which increased during head-up position. Panel (c) shows the mean trend of the instantaneous correlation $\rho_{\mathrm{S}}(k, t)$ between the power spectral density functions derived from HRV and PRV. In the same panel we reported

**Table 2.** Time-invariant analysis results.

| Condition | Index | HRV | PRV | difference ($\overline{\delta_1(k)}$) | $p$ ($t$-test) | Correlation ($\rho_1$) |
|---|---|---|---|---|---|---|
| Supine ($w_1$) | NN (s) | $0.988 \pm 0.195$ | $0.988 \pm 0.195$ | $-0.000\,38 \pm 0.001\,33$ | 0.995 | 1.000 |
| | SDNN (s) | $0.056 \pm 0.022$ | $0.057 \pm 0.022$ | $0.000\,64 \pm 0.001\,87$ | 0.933 | 0.997 |
| | RMSSD (s) | $0.049 \pm 0.028$ | $0.05 \pm 0.027$ | $0.000\,26 \pm 0.001\,86$ | 0.978 | 0.998 |
| | pNN50 (%) | $24.509 \pm 19.151$ | $23.819 \pm 18.067$ | $-0.689\,69 \pm 2.313\,89$ | 0.915 | 0.994 |
| | LF ($s^{-2}$) | $0.002 \pm 0.001$ | $0.002 \pm 0.002$ | $0.000\,09 \pm 0.000\,15$ | 0.859 | 0.997 |
| | HF ($s^{-2}$) | $0.001 \pm 0.001$ | $0.001 \pm 0.001$ | $0.000\,08 \pm 0.000\,13$ | 0.840 | 0.996 |
| | LF (n.u) | $0.657 \pm 0.164$ | $0.653 \pm 0.159$ | $-0.004\,67 \pm 0.015\,86$ | 0.933 | 0.996 |
| | HF (n.u.) | $0.343 \pm 0.164$ | $0.347 \pm 0.159$ | $0.004\,67 \pm 0.015\,86$ | 0.933 | 0.996 |
| | LF/HF (n.u.) | $2.652 \pm 1.834$ | $2.531 \pm 1.718$ | $-0.120\,34 \pm 0.196\,07$ | 0.845 | 0.996 |
| Upright ($w_2$) | NN (s) | $0.787 \pm 0.151$ | $0.788 \pm 0.151$ | $0.001\,16 \pm 0.002\,81$ | 0.982 | 1.000 |
| | SDNN (s) | $0.056 \pm 0.031$ | $0.058 \pm 0.031$ | $0.001\,53 \pm 0.002\,56$ | 0.886 | 0.997 |
| | RMSSD (s) | $0.036 \pm 0.025$ | $0.038 \pm 0.024$ | $0.002\,53 \pm 0.001\,95$ | 0.765 | 0.998 |
| | pNN50 (%) | $13.72 \pm 15.429$ | $15.307 \pm 16.572$ | $1.586\,88 \pm 2.322\,06$ | 0.774 | 0.992 |
| | LF ($s^{-2}$) | $0.006 \pm 0.007$ | $0.006 \pm 0.008$ | $0.000\,33 \pm 0.000\,44$ | 0.899 | 1.000 |
| | HF ($s^{-2}$) | $0.001 \pm 0.001$ | $0.002 \pm 0.002$ | $0.0003 \pm 0.000\,38$ | 0.565 | 0.981 |
| | LF (n.u) | $0.765 \pm 0.194$ | $0.719 \pm 0.206$ | $-0.045\,22 \pm 0.051\,37$ | 0.515 | 0.969 |
| | HF (n.u.) | $0.235 \pm 0.194$ | $0.281 \pm 0.206$ | $0.045\,22 \pm 0.051\,37$ | 0.515 | 0.969 |
| | LF/HF (n.u.) | $6.593 \pm 5.438$ | $5.073 \pm 4.355$ | $-1.519\,94 \pm 2.182\,02$ | 0.375 | 0.924 |
| Supine ($w_3$) | NN (s) | $1.008 \pm 0.193$ | $1.01 \pm 0.195$ | $0.001\,47 \pm 0.0041$ | 0.983 | 1.000 |
| | SDNN (s) | $0.057 \pm 0.025$ | $0.057 \pm 0.024$ | $-0.000\,29 \pm 0.004\,58$ | 0.972 | 0.984 |
| | RMSSD (s) | $0.049 \pm 0.03$ | $0.049 \pm 0.025$ | $-0.000\,42 \pm 0.008\,41$ | 0.965 | 0.970 |
| | pNN50 (%) | $23.949 \pm 18.521$ | $25.506 \pm 18.399$ | $1.557\,52 \pm 2.024\,52$ | 0.807 | 0.994 |
| | LF ($s^{-2}$) | $0.001 \pm 0.001$ | $0.001 \pm 0.001$ | $0.000\,04 \pm 0.000\,09$ | 0.932 | 0.998 |
| | HF ($s^{-2}$) | $0.001 \pm 0.001$ | $0.001 \pm 0.001$ | $0.000\,06 \pm 0.000\,11$ | 0.864 | 0.996 |
| | LF (n.u) | $0.568 \pm 0.201$ | $0.558 \pm 0.201$ | $-0.010\,14 \pm 0.018\,99$ | 0.884 | 0.996 |
| | HF (n.u.) | $0.432 \pm 0.201$ | $0.442 \pm 0.201$ | $0.010\,14 \pm 0.018\,99$ | 0.884 | 0.996 |
| | LF/HF (n.u.) | $1.843 \pm 1.324$ | $1.739 \pm 1.215$ | $-0.103\,94 \pm 0.243\,64$ | 0.813 | 0.985 |

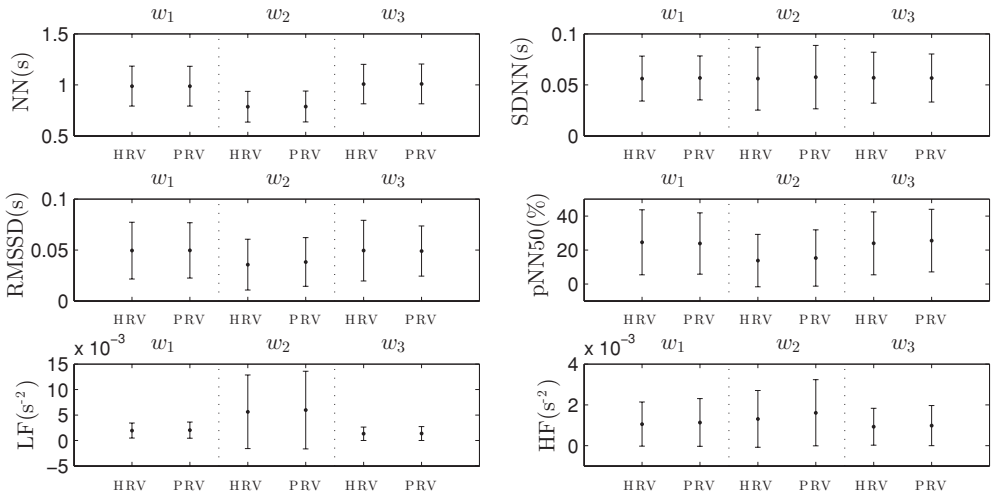


**Figure 3.** Mean ± SD of NN, SDNN, RMSSD, pNN50, $P_{\mathrm{LF}}$ and $P_{\mathrm{HF}}$ derived from HRV and PRV within each window $w_i$.

$\rho_{\mathrm{S}}(k=1,t)$ for the subject who presented the highest number of artefacts in the PPG signal (subject $k=1$). It is shown that artefacts provoked an abrupt decrease in $\rho_{\mathrm{S}}(k,t)$. Panel (d) shows the band coherence $\gamma^2_{\mathrm{B}}(k,t)$ in each spectral band.

Concerning the simulation study, when the location error $\xi_j$ was uniformly distributed between $\pm 8$ ms (std $= 4.9$ ms), HF coherence took similar values as those reported for real data, $\overline{\gamma^2_{\mathrm{HF}}(k,t)} = 0.89$. The results for simulation study with this level of noise, obtained by averaging among subjects are shown in figure 6. Note that, in this case, the isolated effect of the simulated jitter in the PPG fiducial point did not introduce a bias in the instantaneous actual error.

### *3.3. Physiological analysis results*

Results of the time-invariant analysis are reported in table 4. It is shown that $P_{\mathrm{LF}}(k)$ significantly increased as response to the orthostatic stress provoked by the head-up tilt. Student's *t*-test presented similar results for both PRV and HRV signals.

Figure 7 shows the results of the time-varying analysis. It is shown that the time-varying *p*-value estimated from HRV and PRV followed the same trend, $p^{\mathrm{HRV}}_{\mathrm{LF}}(t)$ and $p^{\mathrm{PRV}}_{\mathrm{LF}}(t)$ being almost equal. The variations observed in $P^{\mathrm{X}}_{\mathrm{LF}}(k,t)$ during the tilt table test, see figure 5(a), made $p^{\mathrm{X}}_{\mathrm{LF}}(t)$ change. First, immediately after the head-up tilt, $p^{\mathrm{X}}_{\mathrm{LF}}(t)$ dramatically decreased; then, during $T_2$, $p^{\mathrm{X}}_{\mathrm{LF}}(t)$ continued gradually diminishing, reaching statistical significance about 2 min later; finally, when the supine position was restored $p^{\mathrm{X}}_{\mathrm{LF}}(t)$ abruptly increased to previous values.

## 4. Discussion

The purpose of this paper was to evaluate the possibility of using the PRV signal as an alternative measurement of the HRV signal in non-stationary conditions. Similar results in the analysis performed on indices derived from $d_{\mathrm{HRV}}(t)$ and on indices derived from $d_{\mathrm{PRV}}(t)$ would

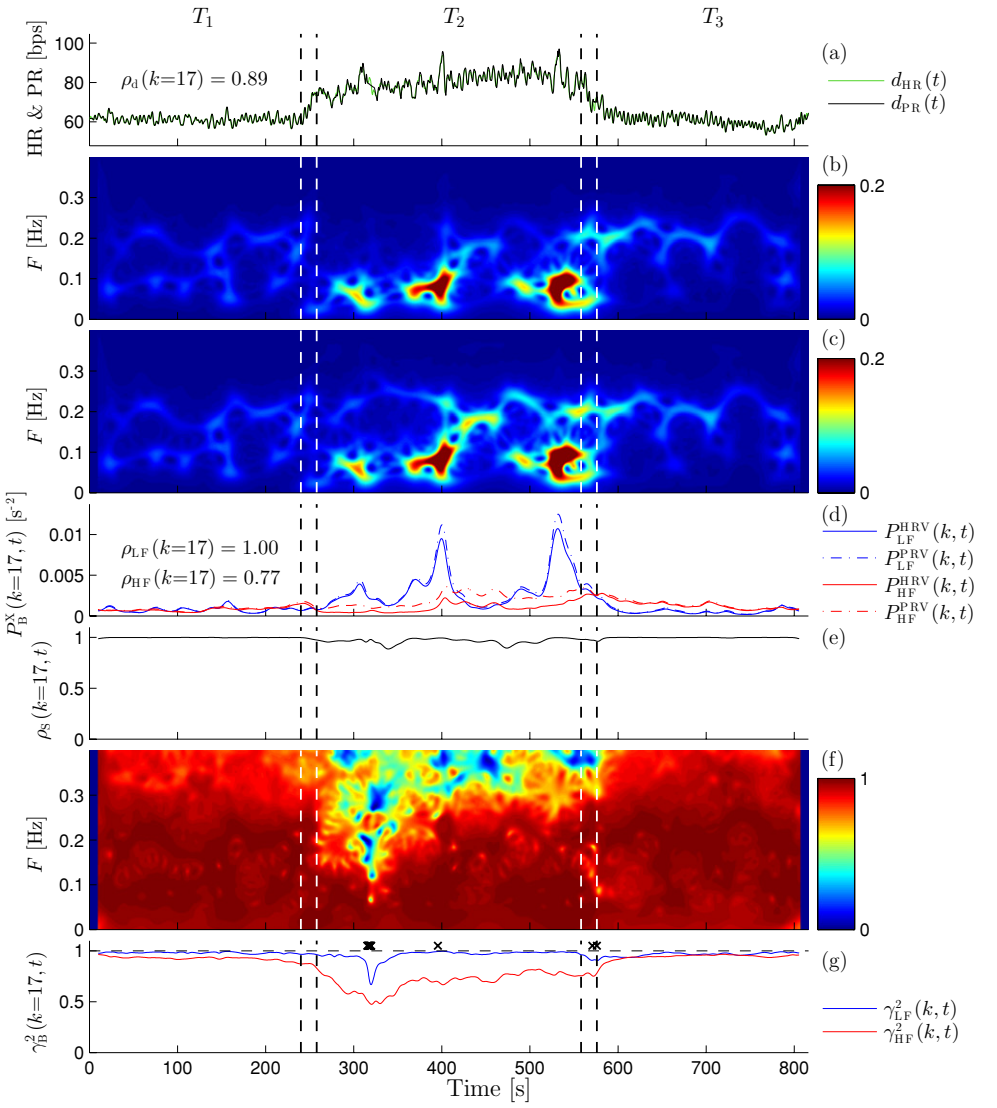


**Figure 4.** Results of TF and TF coherence analysis for subject $k = 17$. (a) Heart rate and pulse rate; (b) TF distribution of $a_{HRV}(t)$; (c) TF distribution of $a_{PRV}(t)$; (d) temporal evolution of the instantaneous power content $P_B^X(k = 17, t)$ within the spectral band B $\in$ {LF, HF} for X $\in$ {HRV, PRV}; (e) correlation coefficient between the instantaneous spectra of the two signals, $\rho_S(k = 17, t)$. (f) TF coherence $\gamma^2(t, f)$ and (g) band coherence $\gamma_B^2(k = 17, t)$. Artefacts in the PPG signal are marked as black crosses.

support the usefulness of the PRV signal as surrogate of the HRV signal. The study is based on the analysis of the changes observed in the heart rate modulation of 17 young subjects during the tilt table test. It consists of three different parts. First, the classical indices of HRV analysis were estimated in three different time epochs during which stationarity was assumed. Second, TF and TF coherence analysis were used to assess and compare the time-varying spectral properties of both signals. Third, we statistically quantified the changes provoked during the experimental procedure with respect to baseline conditions using both the HRV and PRV signals.

**Table 3.** Pearson's correlation $\rho_{\mathrm{I}}(k)$ between time-varying indices $P_{\mathrm{LF}}(k,t)$, $P_{\mathrm{HF}}(k,t)$, $R_{\mathrm{LF/HF}}(k,t)$ for each subject $k$.

| $k$ | 1 | 2 | 3 | 4 | 5 | 6 | 7 | 8 | 9 | 10 | 11 | 12 | 13 | 14 | 15 | 16 | 17 | **MEAN** |
|---|---|---|---|---|---|---|---|---|---|---|---|---|---|---|---|---|---|---|
| $\rho_{\mathrm{LF}}(k)$ | 0.84 | 0.95 | 0.99 | 1 | 1 | 0.99 | 1 | 1 | 1 | 1 | 0.99 | 0.99 | 1 | 1 | 1 | 1 | 1 | $\mathbf{0.98 \pm 0.04}$ |
| $\rho_{\mathrm{HF}}(k)$ | 0.95 | 0.86 | 0.99 | 0.98 | 0.93 | 0.95 | 0.98 | 0.99 | 0.95 | 0.99 | 0.99 | 0.95 | 0.91 | 0.95 | 0.98 | 1 | 0.77 | $\mathbf{0.95 \pm 0.06}$ |
| $\rho_{\mathrm{LF/HF}}(k)$ | 0.89 | 0.99 | 0.96 | 0.99 | 0.98 | 0.97 | 0.99 | 1 | 0.97 | 0.99 | 0.97 | 0.98 | 0.99 | 0.98 | 0.99 | 1 | 0.91 | $\mathbf{0.97 \pm 0.03}$ |

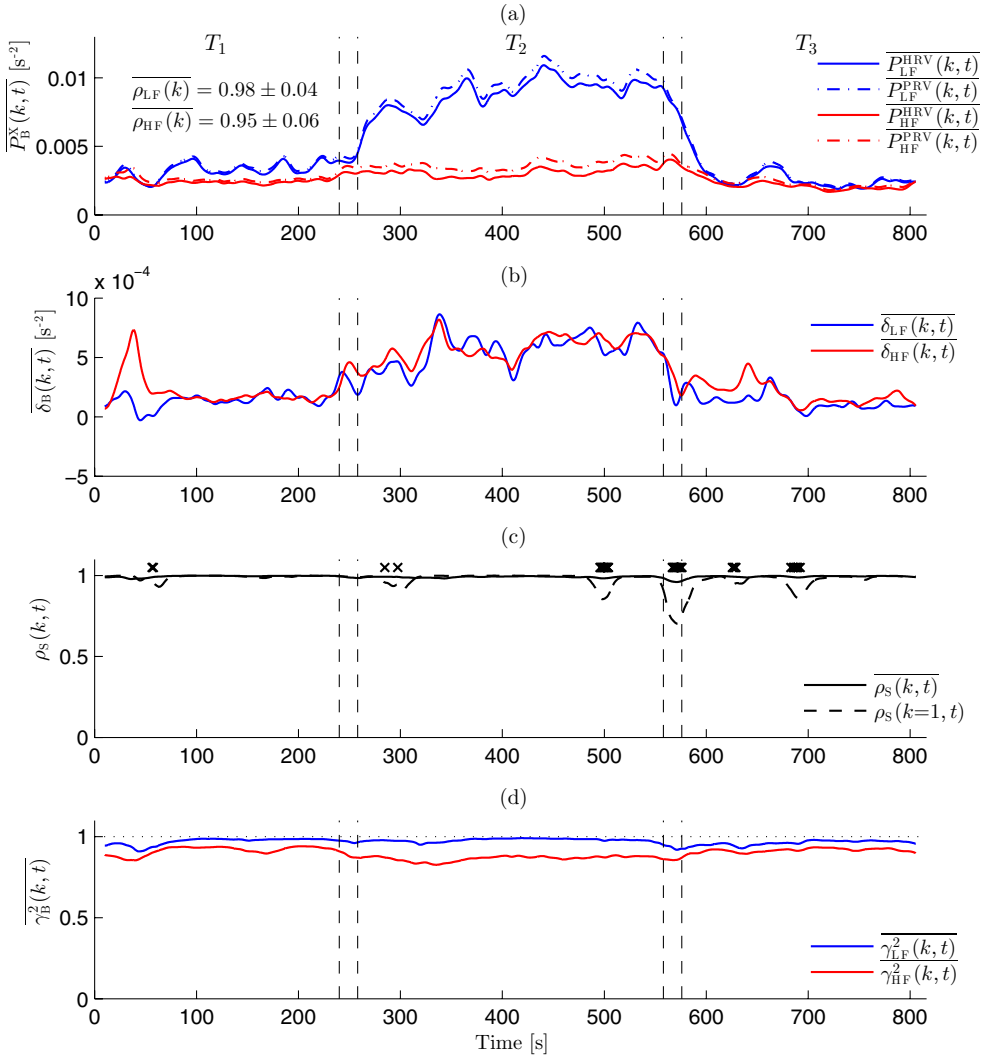


**Figure 5.** Mean trend estimated by averaging among subjects. (a) Temporal evolution of the instantaneous power in each frequency band from HRV (continuous line) and PRV (dash-dotted line); (b) instantaneous actual error in the LF band (red line) and HF band (blue line); (c) mean trend of the instantaneous correlation $\rho_{\mathrm{S}}(k,t)$ between the power spectral density functions derived from HRV and PRV (solid line). The index $\rho_{\mathrm{S}}(k=1,t)$ and artefacts in PPG for subject 1 are reported by the dashed lines and cross marks, respectively and (d) band coherence.

### *4.1. Time-invariant analysis*

A comparison between the classical HRV and PRV analysis during the tilt table test was presented. Table 2 and figure 3 show that classical time and frequency indices derived from PRV presented similar values to the indices derived from HRV, with no statistically significant differences between them ($p > 0.05$) and strong linear correlation ($\rho_{\mathrm{I}} > 0.9$). Generally, during early and later supine position we observed a higher similarity between these indices than during head-up position. Additionally, a positive bias in the estimation of the power

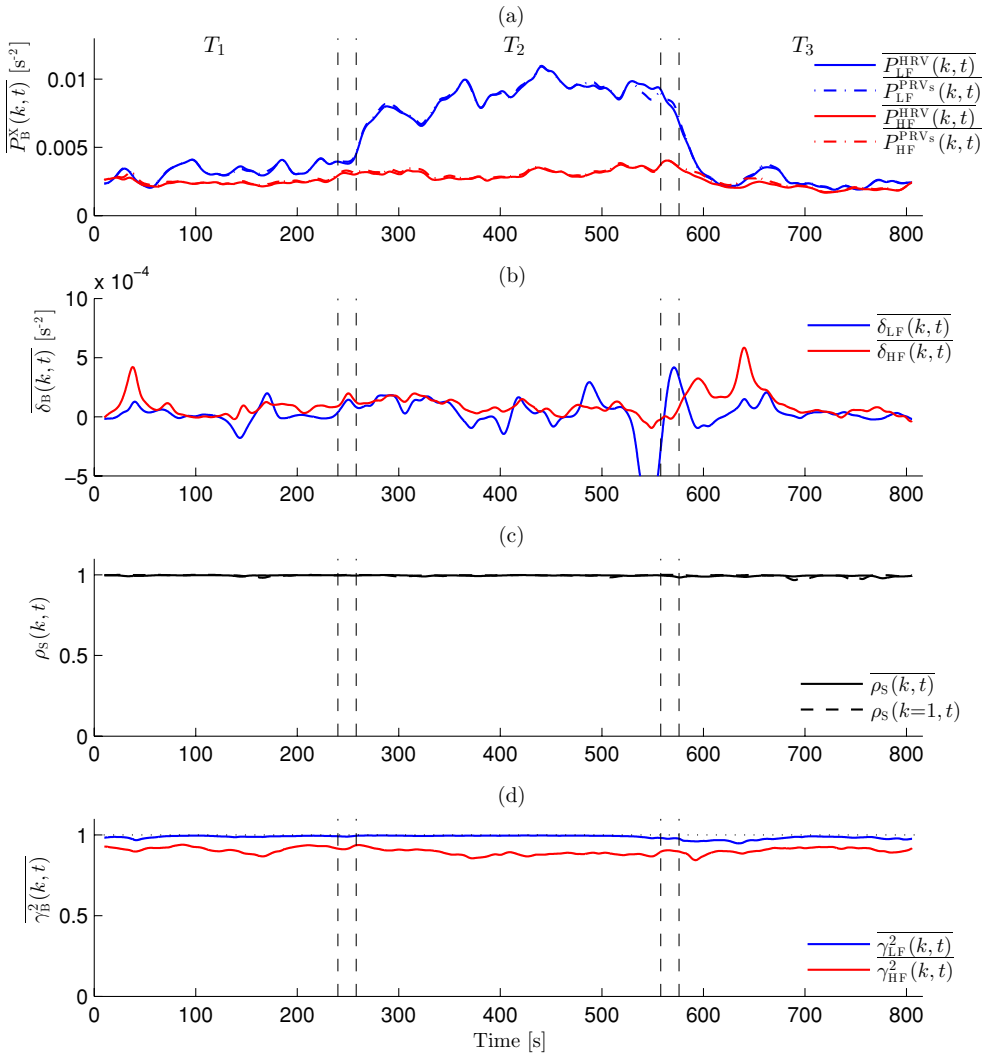


**Figure 6.** Mean trend estimated by averaging among subjects for the simulation study. (a) Temporal evolution of the instantaneous power in each frequency band from HRV (continuous line) and PRV$_{\mathrm{s}}$ (dash-dotted line); (b) instantaneous actual error in the LF band (red line) and HF band (blue line); (c) mean trend of the instantaneous correlation $\rho_{\mathrm{S}}(k,t)$ between the power spectral density functions derived from HRV and PRV$_{\mathrm{s}}$ (solid line). The index $\rho_{\mathrm{S}}(k=1,t)$ for subject 1 is reported by the dashed lines and (d) band coherence.

content from PRV is always present. As already pointed out by Charlot *et al* (2009), Constant *et al* (1999), this bias increases during head-up tilt. This can be due to the effect of PTT, and this point will be discussed in the following section. The results of the time-invariant analysis are in agreement with previous works (Lu *et al* 2008, 2009a, Hayano *et al* 2005, Selvaraj *et al* 2008, Bolanos *et al* 2006, Charlot *et al* 2009) which suggested that PRV could be used as an alternative measurement of HRV during stationary conditions, at least in a resting position (Charlot *et al* 2009). However, in a study with children (Constant *et al* 1999), it was pointed out that the differences observed in the HF band should be carefully considered.

**Table 4.** Time-invariant physiological analysis results ($p$ values). Results of Student's $t$-test for time-invariant analysis comparing each pair of windows $w$.

| $P_{\mathrm{LF}}^{\mathrm{HRV}}$ | $w_1$ | $w_2$ | $w_3$ | $P_{\mathrm{HF}}^{\mathrm{HRV}}$ | $w_1$ | $w_2$ | $w_3$ |
|---|---|---|---|---|---|---|---|
| $w_1$ | 1 | **0.047** | 0.207 | $w_1$ | 1 | 0.569 | 0.7 |
| $w_2$ | – | 1 | **0.021** | $w_2$ | – | 1 | 0.352 |
| $w_3$ | – | – | 1 | $w_3$ | – | – | 1 |
| $P_{\mathrm{LF}}^{\mathrm{PRV}}$ | $w_1$ | $w_2$ | $w_3$ | $P_{\mathrm{HF}}^{\mathrm{PRV}}$ | $w_1$ | $w_2$ | $w_3$ |
| $w_1$ | 1 | **0.046** | 0.194 | $w_1$ | 1 | 0.342 | 0.677 |
| $w_2$ | – | 1 | **0.02** | $w_2$ | – | 1 | 0.184 |
| $w_3$ | – | – | 1 | $w_3$ | – | – | 1 |

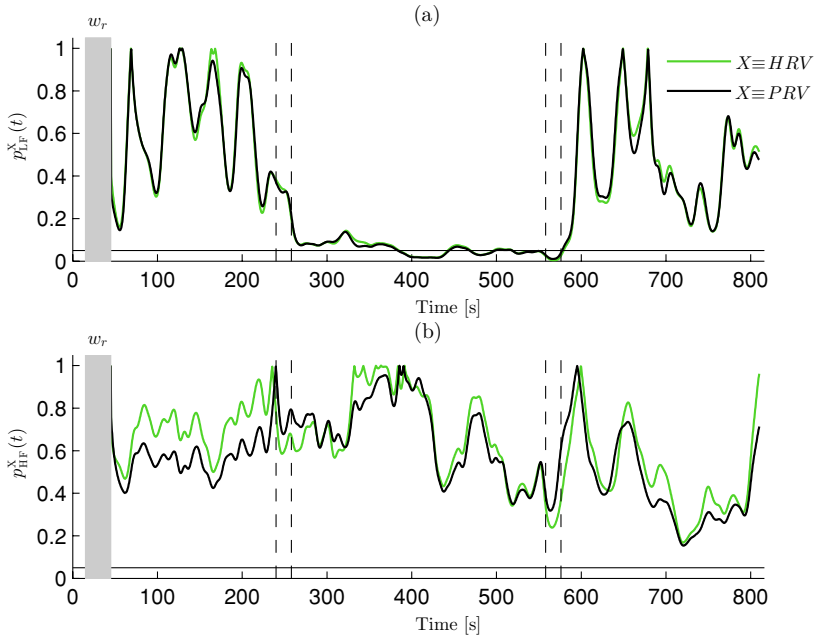


**Figure 7.** Time-varying physiological analysis results. Temporal evolution of (a) the $p$-value $p_{\mathrm{LF}}^{\mathrm{X}}(t)$ and (b) $p_{\mathrm{HF}}^{\mathrm{X}}(t)$, which quantify the differences between the actual values of $P_{\mathrm{B}}^{\mathrm{X}}(k,t)$ and baseline values, for X $\in$ {HRV, PRV} and B $\in$ {LF, HF}. Baseline values were estimated in the reference window marked as grey area, $w_r$.

### *4.2. Time-varying analysis*

Different TF and time-varying approaches have been proposed in the literature to quantify the dynamics of the HRV signal in non-stationary conditions (Mainardi 2009). In this paper we used the SPWVD since it is characterized by a high TF resolution and gives the possibility of performing an independent filtering in both time and frequency. The SPWVD has been used for the assessment of the time-varying spectral properties of HRV during different non-stationary conditions (Jasson *et al* 1997, Akselrod *et al* 1997, Bailón *et al* 2007, Mendez *et al* 2008, Gil *et al* 2009, Orini *et al* 2010) and has been considered as the best option for

analysis of non-stationary HRV signals in a comparative study (Pola *et al* 1996). The choice of the kernel proposed in equation (9) was motivated by the results of Orini *et al* (2009), in which it was used to robustly estimate the TF coherence. In our work, the degree of TF filtering (and interference terms reduction) was sufficient to provide a consistent estimation of the TF coherence, i.e. $\gamma^2(t, f) \in [0, 1]\ \forall(t, f)$, for all subjects.

During the tilt table test we observed high similarity between the patterns of response of the HRV and PRV signals. The global results reported in figure 5 show that the instantaneous power content of the PRV was slightly higher ($\overline{\delta_{\mathrm{B}}(k,t)} < 10^{-3}$ s$^{-2}$) than the instantaneous power content of the HRV signal. The temporal evolution of the index $\delta_{\mathrm{B}}(k,t)$ was almost the same in both frequency bands: during early and later supine position $\overline{\delta_{\mathrm{B}}(k,t)} < 0.25 \times 10^{-3}$ s$^{-2}$, whereas during head-up position $\overline{\delta_{\mathrm{B}}(k,t)}$ increased up to a value of about $0.7 \times 10^{-3}$ s$^{-2}$. It is worth noting that during the highest non-stationary intervals (i.e. transitions where table was tilting), $\delta_{\mathrm{B}}(k,t)$ did not increase. As reported in table 3, their temporal evolution was highly correlated, i.e. $P_{\mathrm{B}}^{\mathrm{HRV}}(k,t)$ and $P_{\mathrm{B}}^{\mathrm{PRV}}(k,t)$ followed the same trend. The correlation between the instantaneous spectral densities of the two signals, $\rho_{\mathrm{S}}(k,t)$, was also very high, being the temporal average of the mean and standard deviation among subjects $0.99 \pm 0.01$. The small decreases of $\rho_{\mathrm{S}}(k,t)$ were due to the presence of some rare artefacts in the PRV signal. The band coherence $\gamma_{\mathrm{B}}^2(k,t)$ showed that, despite of non-stationary conditions, the degree of linear coupling between the two signals was constant during time, and no relevant variations were observed even during upward and downward tilting. Band coherence in LF fluctuated around $0.97 \pm 0.04$ during the entire experimental procedure, while band coherence in HF fluctuated around $0.92 \pm 0.06$ and $0.87 \pm 0.10$ during supine ($T_1$ and $T_3$) and head-up tilt ($T_2$) position, respectively ($0.89 \pm 0.08$ during the entire experimental procedure).

In both time-invariant and time-varying analysis, we observed a positive bias in the measurement of spectral indices from PRV. This bias was observed to increase during head-up tilt. Differences between PRV and HRV are due to the PTT variability and to the variability of the error in the location of the PPG fiducial point, see equation (4). Our hypothesis is that this bias could be due to the variability introduced by PTT, which could be higher during head-up position, because there is no reason to expect an increase in the error in the location of the PPG fiducial point during head-up position. Moreover the lower values observed in $\gamma_{\mathrm{HF}}^2(k,t)$ with respect to $\gamma_{\mathrm{LF}}^2(k,t)$ suggest that, due to the PTT variability, respiration is slightly differently represented in PRV than in HRV, in agreement with Constant *et al* (1999). Time-varying spectral indices estimated from PRV and HRV analyses did follow the same temporal patterns. Nevertheless, small differences exist between their values, mainly in the respiratory band. Thus, when a study aims at accurately estimating these time-varying spectral indices, caution should be used in replacing HRV by PRV. These differences are related to the PTT variability. The TF description of PTT variability goes beyond the purposes of this paper, but further studies on this subject are needed.

Equation (4) describes the relationship between HRV and PRV and shows that the PTT variability as well as the variability of the jitter in the PPG fiducial point makes this relationship non-linear. Given this relationship, and to better understand our results, a simulation study was carried out. We simulated that the difference between HRV and PRV is only due to the jitter in the PPG fiducial point. When $\xi_j$ was uniformly distributed between $\pm 8$ ms (std $=$ 4.9 ms), HF band coherence took similar values as those reported in real data. In addition, this simulation study also showed that the jitter in the PPG fiducial point does not introduce a bias in the instantaneous actual error $\delta_{\mathrm{B}}(k,t)$. This observation corroborates the hypothesis which suggests that the difference between PRV and HRV showed in figure 5(b) is mainly due to the PTT variability.

### *4.3. Physiological analysis*

From both time-invariant and time-varying analysis, we observed a statistically significant increase of the power content in the LF band of HRV and PRV during head-up position. Results of table 4 show that differences in $P^{\mathrm{X}}_{\mathrm{LF}}(k)$ during $w_2$ and $w_3$ were statistically higher than differences during $w_2$ and $w_1$. Simultaneous inspection of figures 5(a) and 7(a) reveals the transient nature of the autonomic response to orthostatic stress. It is shown that the variations in $P^{\mathrm{X}}_{\mathrm{LF}}(k,t)$ provoke changes in the temporal pattern of $p$-values. First, immediately after the head-up tilt, $p^{\mathrm{X}}_{\mathrm{LF}}(t)$ dramatically decreased; then, during $T_2$, $p^{\mathrm{X}}_{\mathrm{LF}}(t)$ continued gradually diminishing, reaching statistical significance about 2 min later; finally, when the supine position was restored $p^{\mathrm{X}}_{\mathrm{LF}}(t)$ abruptly increased to previous values. Moreover, as also shown in figure 7(a) the power content within the LF band during early and later supine positions did not present any relevant difference, pointing out that the recovery was fast. The power content in the HF band did not present any significant change.

Finally, it is worth noting that there was agreement between the physiological analysis based on HRV and PRV. This suggests that in this particular test PRV could be used as a surrogate measurement of HRV to evaluate the autonomic modulation changes of the heart rate for both stationary and non-stationary analysis.

### *4.4. Limitations*

It is well established that PPG measurements are quite sensitive to patient and/or probe-tissue movement artefact (Allen 2007). The presence of motion artefacts is one of the most important limitations of the use of the PRV signal as surrogate of the HRV signal (Lu and Yang 2009). Thus, the automatic artefact detection (Gil *et al* 2008, Yan *et al* 2005, Hayes and Smith, 2001) and replacement of correspondent corrupted signal segments are essential in PPG signal processing. In this study, a PPG artefact detector based on Hjorth parameters was used and subsequently the PPG and ECG signals were manually supervised. The effect of errors in beat and pulse detection was corrected following the algorithm presented by Mateo and Laguna (2003). Artefacted PPG pulses represented less than 1% of total pulses and, thanks to their detection and correction, did not significantly affected our global results. Nevertheless, their effect on the similarity indices of single subjects was still visible. In subject 17 an artefact provoked the decrease observed in TF coherence around 320 s (see figure 4). The PPG recording of subject 1 was most corrupted by artefacts. In figure 5(c), it is shown that artefacts provoked a decrease in the index $\rho_{\mathrm{S}}(k,t)$, being the most relevant decrease associated with artefacts during the downward motion of the automatic table (around 570 s). As also reported by Charlot *et al* (2009), Lu and Yang (2009), high PPG signal quality and robust artefact removal are necessary for accurate PRV analysis.

The accuracy in detecting the fiducial point in PPG $\left(t_{\mathrm{P}_j}\right)$ is also essential in PRV analysis. It mainly depends on the sampling frequency and morphology of the PPG pulse wave. According to Merri *et al* (1990), a low sampling frequency produces an increase in the power of the high-frequency band (generally at least 500 Hz is required to avoid some serious errors). In this study, the PPG signal was sampled at 250 Hz and later it was interpolated using cubic splines up to an equivalent sampling frequency of 1000 Hz in order to match the time resolution of HRV.

The PPG pulse wave is less sharp than the R-wave in ECG, which could introduce some inaccuracy in $t_{\mathrm{P}_j}$ detection. The effect of this error has been introduced in equation (3) by means of the stochastic variable $\xi_j$. The simulation study, which aimed at assessing the isolated effect of these inaccuracies, pointed out that the temporal jitter was not able to reproduce the

bias observed in figure 5(b). If the morphology of the PPG pulse wave does not change along the recording, as in our data, the main difference between PRV and HRV will be due to the PTT variability, according to equation (4). If PPG pulse wave morphology changes, other methods less sensitive to morphology for detecting $t_{P_j}$ as for example methods based on mass centre should be considered, so taking into account the stability of the fiducial point on PPG is important for PRV analysis in each application.

An important point to stress is that during tilt, the ANS reacts in such a way to keep blood pressure values as close as possible to the rest values. If some hypotensive events occur during tilt, they are related to pre-syncopal/syncopal events which did not happen in our data. Thus changes in PRV could not be addressed to hypotensive events in our work.

In this study, beat detections from ECG have been used for determining the temporal location of each pulse wave in PPG. A robust automatic detector of pulses from PPG independent from ECG and adapted to different possible kinds of pulse wave morphology is needed for the application of PRV analysis in clinical routine. An extended study including more subjects and other physiological events associated with non-stationary conditions would be desirable to confirm our results. In addition, a study of the effect of aging as well as of changes in blood pressure on PRV would be interesting. It is well known that older subjects have increasing arterial stiffness, which results in increasingly faster pulse transmission to the periphery (Allen and Murray 2002). Thus, differences between HRV and PRV, which are mainly produced by PTT, could be dependent on aging.

## 5. Conclusion

Classical indices for time-invariant analysis derived from PRV presented similar values to the indices derived from HRV, with no statistically significant differences between them ($p > 0.05$) and strong linear correlation ($\rho_{\mathrm{I}} > 0.97$), in agreement with previous works which suggest that PRV could be used as an alternative measurement of HRV during stationary conditions. In addition, a comparison of time-varying analysis based on the SPWVD was carried out in order to evaluate the usefulness of PRV as a surrogate measurement of HRV during non-stationary conditions. We observed that instantaneous power contents estimated from HRV and PRV were highly correlated ($0.98 \pm 0.04$ and $0.95 \pm 0.06$ for the LF and HF bands respectively) and their differences were small ($\overline{\delta_{\mathrm{B}}(k,t)} < 10^{-3}$ s$^{-2}$); the TF spectra of both signals were highly correlated ($0.99 \pm 0.01$); TF coherence in the LF and HF bands was high ($0.97 \pm 0.04$ and $0.89 \pm 0.08$, respectively). Finally, a physiological analysis to evaluate the autonomic modulation changes of heart rate during the tilt table test showed that the same conclusions could be inferred from HRV and PRV analysis.

Our results indicate that there are some small differences in the time-varying spectral indices extracted from HRV and PRV, mainly in the respiratory band. Nevertheless, these differences were sufficiently small to suggest the use of the PRV signal as an alternative measurement of the HRV signal during non-stationary conditions, at least during the tilt table test. Finally, we pointed out that these differences are related to the PTT variability.

## Acknowledgments

This work was partially supported by Ministerio de Ciencia y Tecnología, FEDER under Project TEC2007-68076-C02-02/TCM; and Diputación General de Aragón (DGA), Spain, through Grupos Consolidados GTC ref:T30. The authors would like to acknowledge Ana Minchole whose work contributed significantly to this research.

## References


Akselrod S, Oz O, Greenberg M and Keselbrener L 1997 Autonomic response to change of posture among normal and mild-hypertensive adults: investigation by time-dependent spectral analysis *J. Autonom. Nerv. Syst.* **64** 33–43

Allen J 2007 Photoplethysmography and its application in clinical physiological measurement *Physiol. Meas.* **28** R1–39

Allen J and Murray A 2002 Age-related changes in peripheral pulse timing characteristics at the ears, thumbs and toes *J. Human Hypertens.* **16** 711–7

Bailón R, Laguna P, Mainardi L and Sörnmo L 2007 Analysis of heart rate variability using time-varying frequency bands based on respiratory frequency *29th Annu. Int. Conf. of the IEEE EMBS* pp 6674–6677

Bernardi L, Solda A R, Coats A J S, Reeder M, Calciati A, Garrard C S and Sleight P 1996 Autonomic control of skin microvessels: assessment by power spectrum of photoplethysmographic waves *Clin. Sci.* **90** 345–55

Bolanos M, Nazeran H and Haltiwanger E 2006 Comparison of heart rate variability signal features derived from electrocardiography and photoplethysmography in healthy individuals *Engineering in Medicine and Biology Society. Proc. of the 28th Annu. Int. Conf. of the IEEE* pp 4289–94

Charlot K, Cornolo J, Brugniaux J V, Richalet J P and Pichon A 2009 Interchangeability between heart rate and photoplethysmography variabilities during sympathetic stimulations *Physiol. Meas.* **30** 1357–69

Chen W, Kobayashi T, Ichikawa S, Takeuchi Y and Togawa T 2000 Continuous estimation of systolic blood pressure using the pulse arrival time and intermittent calibration *Med. Biol. Eng. Comput.* **38** 569–74

Constant I, Laude D, Murat I and Elghozi J L 1999 Pulse rate variability is not a surrogate for heart rate variability *Clin. Sci.* **97** 391–7

Costa A and Boudreau-Bartels G 1995 Design of time-frequency representations using a multiform, tiltable exponential kernel *IEEE Trans. Signal Process.* **43** 2283–301

Foo J Y A and Lim C S 2006 Pulse transit time as an indirect marker for variations in cardiovascular related reactivity *Technol. Health Care* **14** 97–108

Gil E, Bailón R, Vergara J M and Laguna P 2010 PTT variability for discrimination of sleep apnea related decreases in the amplitude fluctuations of PPG signal in children *IEEE Trans. Biomed. Eng.* **57** 1079–88

Gil E, Mendez M O, Vergara J M, Cerutti S, Bianchi A M and Laguna P 2009 Discrimination of sleep apnea related decreases in the amplitude fluctuations of PPG signal in children by HRV analysis *IEEE Trans. Biomed. Eng.* **56** 1005–14

Gil E, Vergara J M and Laguna P 2008 Detection of decreases in the amplitude fluctuation of pulse photoplethysmography signal as indication of obstructive sleep apnea syndrome in children *Biomed. Signal Process. Control* **3** 267–77

Hayano J, Barros A K, Kamiya A, Ohte N and Yasuma F 2005 Assessment of pulse rate variability by the method of pulse frequency demodulation *BioMed. Eng. Online* **4** 62

Hayes M J and Smith P R 2001 A new method for pulse oximetry possessing inherent insensitivity to artifact *IEEE Trans. Biomed. Eng.* **48** 452–61

Hertzman A B 1938 The blood supply of various skin areas as estimated by the photo-electric plethysmograph *Am. J. Physiol* **124** 328–40

Hlawatsch F 1991 Duality and classification of bilinear time-frequency signal representations *IEEE Trans. Signal Process.* **39** 1564–74

Jasson S, Médigue C, Maison-Blanche P, Montano N, Meyer L, Vermeiren C, Mansier P, Coumel P, Malliani A and Swynghedauw B 1997 Instant power spectrum analysis of heart rate variability during orthostatic tilt using a time/frequency domain method *Circulation* **96** 3521–6

Julu P O O, Cooper V L, Hansen S and Hainsworth R 2003 Cardiovascular regulation in the period preceding vasovagal syncope in conscious humans *J Physiol.* **549** 299–311

Khanokh B, Slovik Y, Landau D and Nitzan M 2004 Sympathetically induced spontaneous fluctuations of the photoplethysmographic signal *Med. Biol. Eng. Comput.* **40** 80–5

Lu G and Yang F 2009 Limitations of oximetry to measure heart rate variability measures *Cardiovasc. Eng.* **9** 119–25

Lu G, Yang F, Taylor J A and Stein J F 2009 A comparison of photoplethysmography and ECG recording to analyse heart rate variability in healthy subjects *J. Med. Eng. Technol.* **33** 634–41

Lu S, Zhao H, Ju K, Shin K, Lee M, Shelley K and Chon K 2008 Can photoplethysmography variability serve as an alternative approach to obtain heart rate variability information? *J. Clin. Monit. Comput.* **22** 23–9

Ma T and Zhang Y T 2006 Spectral analysis of pulse transit time variability and its coherence with other cardiovascular variabilities *Proc. of the 28th Annu. Int. Conf. of the IEEE EMBS* pp 996–9

Mainardi L T 2009 On the quantification of heart rate variability spectral parameters using time-frequency and time-varying methods *Phil. Trans. R. Soc.* A **367** 255–75

Malliani A, Pagani M, Lombardi F and Cerutti S 1991 Cardiovascular neural regulation explored in the frequency domain *Circulation* **84** 482–92

Martin W and Flandrin P 1985 Wigner–Ville spectral analysis of nonstationary processes *IEEE Trans. Acoust. Speech Signal Process.* **33** 1461–70

Martin W A, Camenzind E and Burkhard P R 2003 ECG artifact due to deep brain stimulation *Lancet* **361** 1431

Martinez J P, Almeida R, Olmos S, Rocha A P and Laguna P 2004 A wavelet-based ECG delineator: evaluation on standard databases *IEEE Trans. Biomed. Eng.* **51** 570–81

Mateo J and Laguna P 2003 Analysis of heart rate variability in the presence of ectopic beats using the heart timing signal *IEEE Trans. Biomed. Eng.* **50** 334–43

Mendelson Y 1992 Pulse oximetry: theory and applications for noninvasive monitoring *Clin. Chemistry* **38** 1601–7

Mendez M O, Bianchi A M, Montano N, Patruno V, Gil E, Mantaras C, Aiolfi S and Cerutti S 2008 On arousal from sleep: time-frequency analysis *Med. Biol. Eng. Comput.* **46** 341–51

Merri M, Farden D C, Mottley J G and Titlebaum E L 1990 Sampling frequency of the electrocardiogram for spectral analysis of the heart rate variability *IEEE Trans. Biomed. Eng.* **37** 99–105

Montano N, Ruscone T G, Porta A, Lombardi F, Pagani M and Malliani A 1994 Power spectrum analysis of heart rate variability to assess the changes in sympathovagal balance during graded orthostatic tilt *Circulation* **90** 1826–31

Naschitz J E *et al* 2004 Pulse transit time by R-wave-gate infrared photoplethysmography: review of the literature and personal experience *J. Clin. Monit. Comput.* **18** 333–42

Nitzan M, Babchenko A, Khanokh B and Landau D 1998 The variability of the photoplethysmographic signal-a potential method for the evaluation of the autonomic nervous system *Physiol. Meas.* **19** 93–102

Orini M, Bailón R, Enk R, Koelsch S, Mainardi L and Laguna P 2010 A method for continuously assessing the autonomic response to music-induced emotions through HRV analysis *Med. Biol. Eng. Comput.* **48** 423–33

Orini M, Bailón R, Mainardi L, Mincholé A and Laguna P 2009 Continuous quantification of spectral coherence using quadratic time-frequency distributions: error analysis and application *Int. Conf. Computers in Cardiology* pp 681–684

Pagani M *et al* 1986 Power spectral analysis of heart rate and arterial pressure variabilities as a marker of sympatho-vagal interaction in man and conscious dogs *Circ. Res.* **59** 178–93

Pola S, Macerata A, Emdin M and Marchesi C 1996 Estimation of the power spectral density in nonstationary cardiovascular time series: assessing the role of the time-frequency representations (TFR) *IEEE Trans. Biomed. Eng.* **43** 46–59

Selvaraj N, Jaryal A K, Santhosh J, Deepak K K and Anand S 2008 Assessment of heart rate variability derived from finger-tip photoplethysmography as compared to electrocardiography *J. Med. Eng. Technol.* **32** 479–84

Task Force 1996 Task Force of The European Society of Cardiology and The North American Society of Pacing and Electrophysiology. Heart rate variability: Standards of measurement, physiological interpretation, and clinical use *European Heart J.* **17** 354–81

White L B and Boashash B 1990 Cross spectral analysis of nonstationary processes *IEEE Trans. Inf. Theory* **36** 830–5

Yan Y, Poon C and Zhang Y 2005 Reduction of motion artifact in pulse oximetry by smoothed pseudo wigner-ville distribution *J. NeuroEng. Rehabil.* **2** 3

Yoshiya I, Shimada Y and Tanaka K 1980 Spectrophotometric monitoring of arterial oxygen saturation in the fingertip *Med. Biol. Eng. Comput.* **18** 27–32